Electrical characterization of micro-organisms using microfabricated devices

H. Chang and A. Ikram
School of Electrical and Computer Engineering, Purdue University, West Lafayette, Indiana 47907-1285

F. Kosari and G. Vasmatzis
Mayo Clinic, Rochester, Minnesota 55905

A. Bhunia
Department of Food Sciences, Purdue University, West Lafayette, Indiana 47907-1285

R. Bashir[a)]
Department of Biomedical Engineering, School of Electrical and Computer Engineering, Purdue University, West Lafayette, Indiana 47907-1285

(Received 10 January 2002; accepted 29 July 2002)

This article describes the electrical characterization of live and heat-inactivated micro-organisms within microstructures. Electrophoretic movement of live and heat-inactivated *Listeria innocua* on interdigitated fingered electrodes confirmed the presence of negative charges on the live micro-organisms and demonstrated positive or neutral charges on the heat-inactivated micro-organisms. A micropore was fabricated in an oxide coated silicon diaphragm, which was placed between two chambers containing ionic buffer solutions. When the micro-organism electrophoretically traversed the pore, the background ionic current was blocked and a decrease in the current was observed. As an initial test case, negatively charged polystyrene beads, which were 2.38 μm in diameter, were electrophoretically driven across the pore. Then, *Listeria innocua*, suspended in tris-glycine buffer, were also moved through the pore and their electrophoretic mobility was determined. In addition, the values of mobility of the micro-organisms through the micropore were found to be about 3 orders of magnitude smaller than their mobility without the pore, which can be explained by the higher hydrostatic pressures experienced by the micro-organisms when traversing through the pore. © *2002 American Vacuum Society.*
[DOI: 10.1116/1.1508805]

I. INTRODUCTION

Biological entities such as cells, proteins, and DNA carry charges and can be made to move under an applied electric field. The drift of these entities has been used as a way to obtain important information such as their charge, length, electrophoretic mobility, etc.[1,2] Such analyses are typically carried out on samples with many entities and the information obtained, such as the mobility, represents an average value for the ensemble. The possible characterization of single entities and molecules is very attractive for conducting basic scientific studies and for practical applications such as ultrasensitive detection and diagnosis.

One approach to such characterization is to produce a device with a single pore that can be used for the characterization of single entities and detection and diagnostic applications. Such devices are made possible through microfabrication based miniature devices that can be used to manipulate single micro-organisms. Numerous *nonelectrical* characterizations of cells in such microstructures have been performed. Ogura *et al.*[3] studied blood cell deformity in 1 μm wide pores made in 0.4 μm thick silicon nitride membranes. Kikuchi *et al.*[4] used anisotropic etching to form 9 μm wide V-groove channels, both for the study of blood rheology and cell deformation. Subsequently, Tracey *et al.*[5] used an anistropically etched V-groove device to show that 8 μm diameter erythrocytes deform and elongate to 10–12 μm length when they are forced through 4 μm wide and deep channels. The cells were moved using hydrodynamic pressure and the device was used to only study the mechanical deformation of cells. No electrical characterization was performed in any of these studies. Brody *et al.*[6,7] used lithographic arrays for cell sorting using microfabricated lattices. A large number of structures in the lattice allowed the sorting of many cells simultaneously and white blood cells were efficiently separated from red blood cells.

Studies have also been reported on the electrical characterization of single cells in microstructures and the use of electronic properties of cells for concentration, transport, and separation. Larsen *et al.*[8] demonstrated the fabrication of a coulter-counter based microscale particle counter. Fluidic operation of the device was completed but no detection results were presented. Ayliffe *et al.*[9] fabricated lateral microchannels with integrated electrodes to directly measure the impedance as a function of frequency of toadfish red blood cells and human neutrophils. The principle of dielectrophoresis has also been used to trap cells in ''potential'' wells set up using different geometries of microfabricated electrodes. Many examples of cell manipulation which include cell trap-

[a)]Electronic mail: bashir@ecn.purdue.edu

ping, sorting, and transport can be found in a review by Fuhr *et al.*[10]

The purpose of this article is to first present the electrical characterization of micro-organisms using interdigitated electrodes, which demonstrated that the negative charge state of live cells is altered when they are heat inactivated. Then the characterization of the cells was performed in microstructures using a coulter-counter based approach, where electronic detection is achieved by the blockage of background ionic current flow upon the passage of the species of interest. Microscale pores were fabricated and polystyrene beads used to test the concept and verify the operation of the device. Then, live and heat-inactivated bacteria *Listeria innocua* were employed as a biological test case for verifying the technique and the feasibility to characterize biological entities. *Listeria innocua* was chosen for this initial study since it is nonpathogenic and hence easier to handle but still bears similarities to *listeria monocytogenous*, a pathogenic species of genus *listeria* known to cause listeriosis in immune-compromised individuals. Current versus time measurements were performed and the translocation times of the beads and *listeria* through the pore were obtained as a function of the applied electric field. Translocation time was used to compute the electrophoretic velocity of beads and *Listeria innocua*, and their mobility through the pore was determined to examine the electrophoretic properties of these charged species. The electrophoretic mobility of live *Listeria innocua* was found to be different in magnitude and polarity than that of dead ones. Microscope video measurements of ''free'' beads and *Listeria innocua* without any pore were performed and compared to the data obtained from beads and *listeria* through the pore. The mobility of beads and bacteria with the pore was found to be 3 orders of magnitude lower than the mobility of free beads and bacteria, due to increased hydrostatic pressure induced on the charged entities in the narrow pore.

The device used herein can have the following applications; (i) to study the movement and charge characteristics of individual entities; (ii) to study the physical, electrical, and chemical interactions between the individual entities (organisms, molecules) and the microfabricated surfaces; (iii) to scale the pore size down so that it can be used as a single molecule detector. The eventual goal of our project is to scale the size of the pore down to nanoscale dimensions so that such a device could be used for direct characterization of DNA and related molecules.

II. MORPHOLOGICAL EVALUATION

Figures 1(a) and 1(b) show optical phase contrast microscope pictures (1000×) of a live and heat-inactivated *Listeria innocua* taken in our laboratory. As can be seen by the micrographs, the live bacteria is structurally intact and has a dense cellular region. The heat inactivated bacteria were exposed to 80 °C for 20 min. They, on the other hand are smaller, do not have a continuous and well-defined cell wall, and have a central region that has clear subregions within. These observations were confirmed earlier by more detailed cross-sectional transmission electron micrographs of *Listeria innocua* treated by pulsed electric fields.[11] In that case, clear and bright regions were observed inside the cells indicating a lack of cytoplasm when the cell membrane was perforated by a high electric field pulse. It can be conjectured that the cell boundary has also been perturbed under our case of heat-inactivation of the cells and that the charge state of the cell will be altered due to changes in the fixed charges on the cell wall. The heat treatment will also denature the proteins on the cell wall and hence could significantly alter the usual cell surface charges.

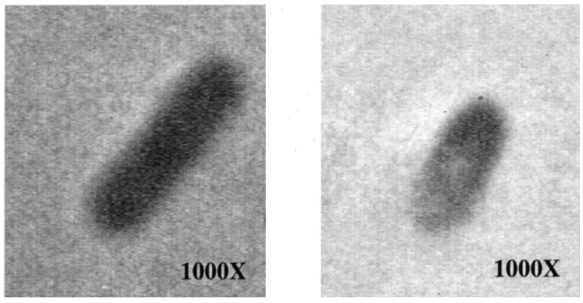

FIG. 1. Phase contrast optical micrographs (1000×) of (a) live *Listeria innocua*, with a well-defined cell wall (b) heat-inactivated *Listeria innocua*, with a noncontinuous cell wall.

III. EXAMINATION OF CHARGE STATE OF CELLS

Live cells are known to have fixed negative charges on the surface of the cell membrane, attributed to the cell wall components such as phosphates, proteins, and carboxylate groups, etc.[12] To examine the charge state of the bacteria, an interdigitated microelectrode device was used. These microscale metallic electrodes were obtained (Abtech Scientific Inc. Richmond, VA). These microelectrodes had an interdigitated layout with line width and spacing of 15 μm. *Listeria innocua* was cultured in Brain Heart Infusion (BHI) broth (Difco Laboratories, Detroit, MI) for 16 h at 37 °C, then washed by centrifugation and resuspension in a low conductivity tris-glycine (tris-gly) buffer to eliminate all the electrolytes present in the culture broth. Tris-gly buffer contains 3.6 mM tris, 4.7 mM glycine, plus 0.05% (vol/vol) tween-20 (a detergent). The detergent is necessary to prevent lumping of the cells. The nominal pH and conductivity of the buffer are 7.4 and 33.5 mS/cm, respectively. After washing, the bacteria were resuspended at concentration of 10^8 cells/ml. Dead *Listeria innocua* was prepared by heating an aliquot of fresh live *Listeria innocua* for 20 min at 80 °C. The cells were fluorescently labeled using the *Bac*light™ kit from Molecular Probes (L-7012 LIVE/DEAD Bacterial Viability Kit).[13] This kit utilizes mixtures of a green-fluorescent nucleic acid stain (SYTO 9) and the red-fluorescent nucleic acid stain (propidium iodide). When used alone, the green-fluorescent stain labels all bacteria, whether their membranes are intact or not. However, the red-fluorescent dye only enters the organism with damaged membranes, causing a re-

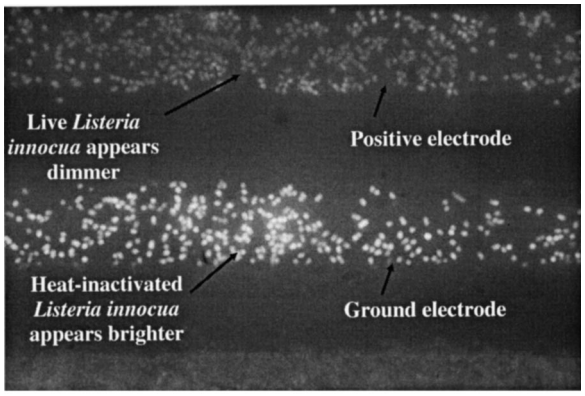

FIG. 2. Fluorescence image of the stained *Listeria innocua* being collected on the interdigitated electrodes. The live listeria is dimmer and the heat-inactivated ones are brighter.

duction in the green fluorescent signal intensity. A 1:1 mixture of these live and dead cells was labeled with the kit, placed on the electrode array and a 1 V dc bias was applied on one of the electrodes while the other electrode was grounded. The wavelength for exciting the red-fluorescent dye was used and it was observed the cells accumulated on the ground electrode were bright red color whereas the cells which accumulated on the positive electrode were not as bright. Figure 2 shows a black and white print of the optical image. Thus, the bright red-green cells were the ones which had compromised membranes (i.e., the heat-inactivated ones) and the green cells (dimmer) were the live ones. The collection on the specific electrodes proved that the live cells mostly accumulated on the positive electrodes and the dead cells mostly accumulated on the adjacent negative electrode. This simple experiment proved the alteration of the charge state of the cells upon heat inactivation. Hence, micropores were designed and fabricated as discussed below to further investigate the charge state of the cells.

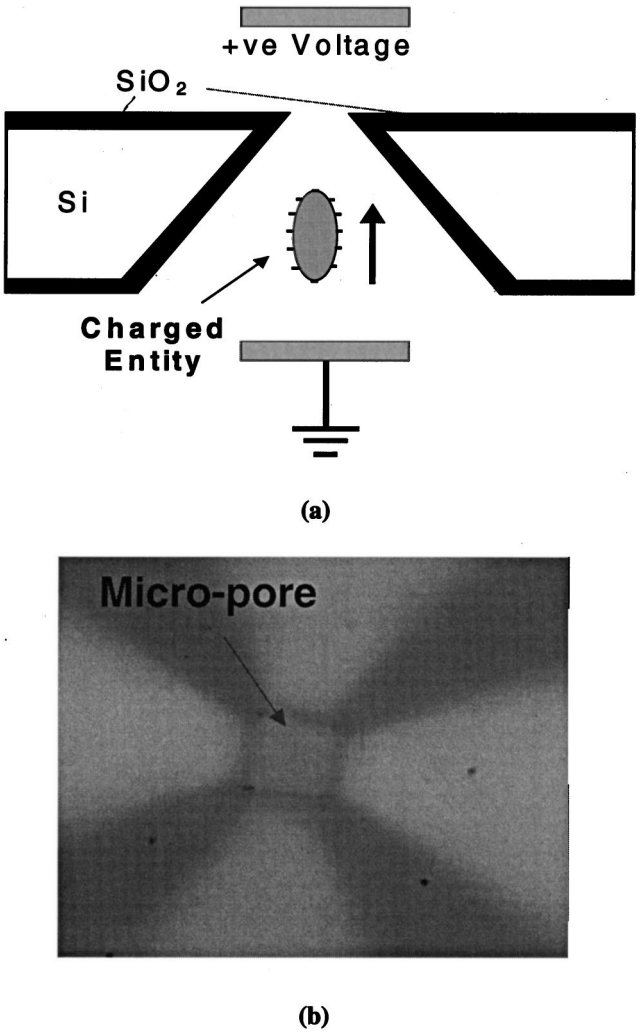

FIG. 3. (a) Final cross section of the device, along with the measurement concept, (b) an optical micrograph of the pore.

IV. MICROPORE FABRICATION AND EXPERIMENTAL DETAILS

The micropore was fabricated using a (100) crystal surface, double-sided-polished silicon wafer. The fabrication commenced with the growth of a 3000 Å oxide in wet ambient at 1050 °C for 45 min. AZ1518 photoresist was patterned on both sides of the wafer and the first mask was used to define a window for wet anisotropic silicon etch from the back side. The anisotropic silicon etch was done using tetramethyl-ammonium-hydroxide (TMAH) and produced a cavity that reached all the way to the front side of the wafer. The angle between the (100) and the (111) plane (54.7°) and the appropriate choice of the size of patterns on the backside of the wafer can be used to produce micropores ranging from 2 by 2 μm to 10 by 10 μm. The oxide was striped and regrown to produce a conformal layer on all exposed surfaces. The wafer was separated into 2 mm by 2 mm chips (partially achieved using the wet TMAH etch), each containing one single pore. The final cross section, along with the device concept is illustrated in Fig. 3(a). Figure 3(b) shows an optical micrograph of the pore. The pore used in the measurements described below was 3.9 μm$\times$4.4 μm. The chip was placed between two Teflon blocks with semicircular channels machined into these blocks. The channel was 2.2 cm long and 4 mm wide and was later filled with buffer solution.

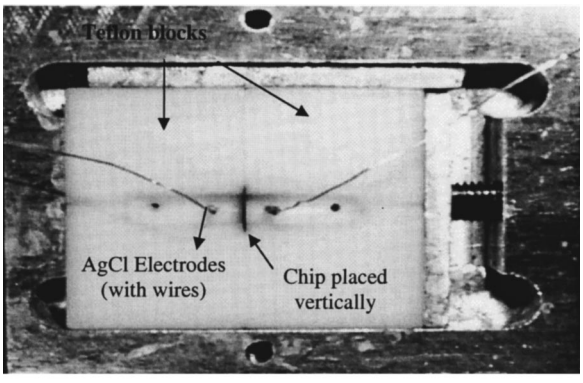

FIG. 4. Image of the measurement apparatus.

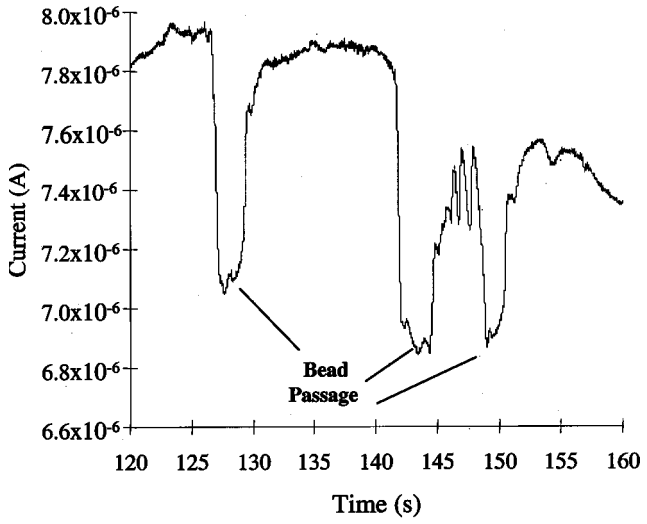

FIG. 5. Typical plot of current variation vs time as the beads traverse through the pore. The voltage applied was 20 V and the bead concentration $=8\times10^9$/ml.

Figure 4 shows the measurement apparatus used for the electrical measurement. Electrodes with silver chloride pellets (World Precision Instrument, Sarasota, FL) were used to apply the voltage and measure the current. The distance between the electrodes was set at 0.5 cm. The electrodes were connected to an HP 4156 semiconductor parameter analyzer capable of doing time sampling measurements, with maximum time and current resolution being 2 ms and 0.01 pA, respectively.

Polystyrene beads, which were 2.38 μm in diameter, were obtained (part PP-20-10, Spherotech, Libertyville, IL). These beads were suspended in Milli-Q water with 0.01% NP 40 (detergent). The concentration of beads used for our measurements was 8×10^9 beads/ml. Before any measurements were performed, the Teflon blocks and the chip were cleaned by a mixture of $H_2SO_4+H_2O_2$. The applied voltage results in the movement of the entities with the fixed charge towards the positive terminal and this phenomenon is identical to electrophoretic movements of DNA, proteins, and cells.

V. MEASUREMENT RESULTS AND DISCUSSION

A typical measurement result with the bead passage is illustrated in Fig. 5. Upon introduction of the beads to the chamber with the negative electrodes, current fluctuations were observed. As the ionic current is blocked by the passage of the entities through the pore, the ionic current decreases. After the entities pass through the pore, the current level increases again. Translocation time was defined as the period between when the current starts to drop and the current recovers to its original level. To analyze the translocation times statistically, all of translocation times were recorded, the maximum and the minimum of the recorded values were eliminated, and remaining values were used to obtain average and standard deviation.

The relationship between the velocity of the moving species ν_p and the applied electric field E is

$$\nu_p=\mu_E E. \tag{1}$$

The velocity of beads is noted as $\nu_p=d/T_{\mathrm{tr}}$, where ν_p is the velocity of the beads in the pore, d is the diameter of the

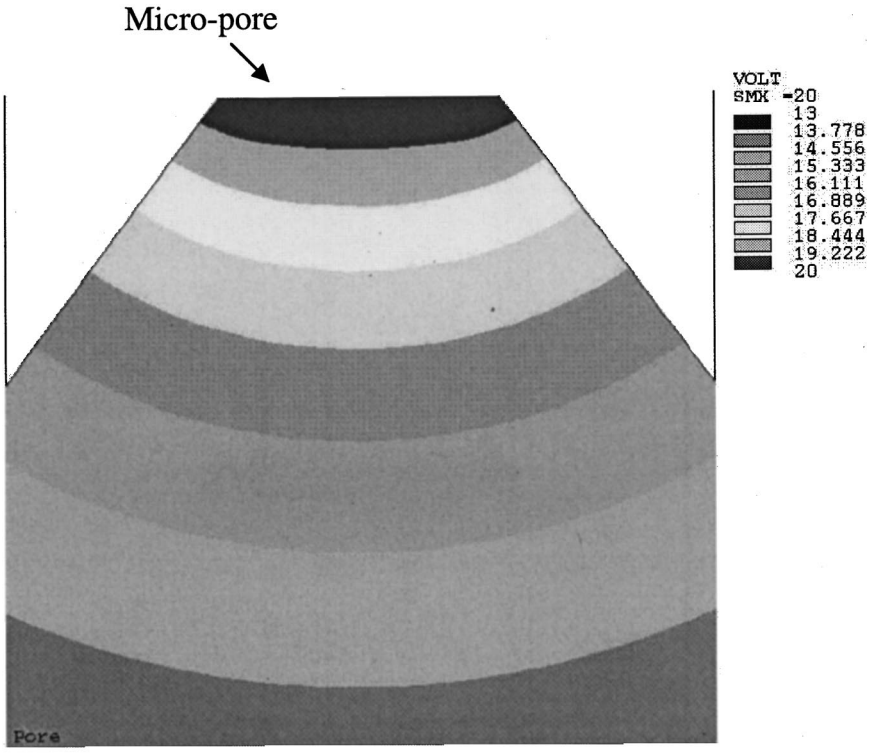

FIG. 6. Simulation results of the electric field near the pore. The top of the figure represents the pore where the electric field is $\sim10^6$ V/m, which is 250 times than V/d.

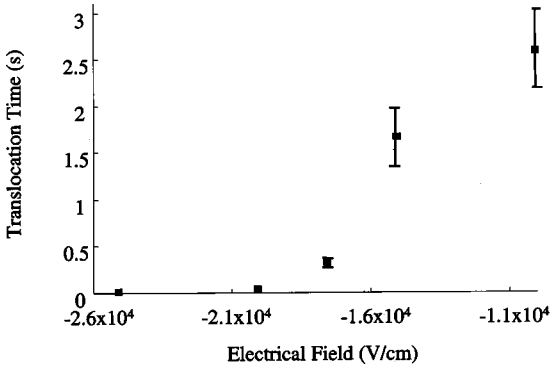

FIG. 7. Plot of translocation time of beads through the pore vs applied electric field.

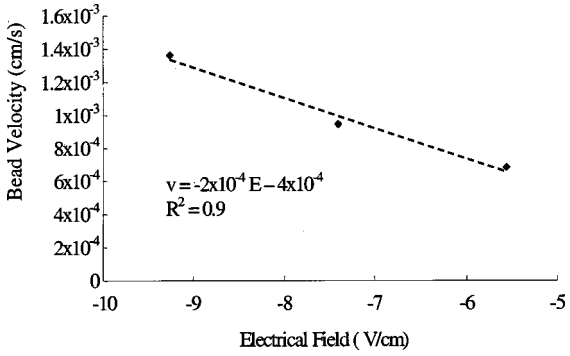

FIG. 9. Average velocity of free beads (without pore) vs the electric field. The slope of the line used to fit the points results in a mobility of -2×10^{-4} cm^2/V s.

bead, and T_{tr} is the translocation time. Since the pore is triangular in shape, as formed by the anisotropic etch, the distance traversed by the beads during the translocation time is the diameter of the bead itself. A plot of velocity versus electric field can then be used to extract the mobility. However, it is important to note that the applied electric field (V/L) is different than the electric field at the pore since the current density increases at the region of interest. To estimate the electric field at the pore, ANSYS (finite element software) was used to simulate the microstructure and obtain the potential contours in the region close to the pore. Figure 6 shows the simulated shape of the voltage potential contours at the pore. These simulated values were used in the extraction of mobility from a plot of velocity as a function of electric field. It can also be noted that the mobility μ_E is related to the equivalent charge Q on the surface of the beads the following equation;[14]

$$\mu_E = Q/6a\pi\eta, \tag{2}$$

where η is the viscosity of buffer solution and a is the radius of a spherical charged entity.

The plot of measured translocation time of beads through the pore versus electric field at the pore is shown in Fig. 7. The translocation time decreases with increasing electric field as expected. The standard deviation in the translocation time was larger for the smaller electric field values presumably due to the larger interactions between the pore and the beads. Figure 8 shows the plot of the average velocity through the pore versus the electric field at the pore. The dependence is linear when the three points at high fields are examined and a least square fit can be used to extract an effective mobility of -2×10^{-6} cm^2/V s. The bead velocity was also obtained from microscopic video measurements in a setup without the chip and pore. Figure 9 shows this result and the velocity versus electric field curve was obtained to extract the mobility of -2×10^{-4} cm^2/V s. In this particular case, the electric field was determined simply by V/L and there was no need to adjust it using simulations. The charge on the bead can be approximated using the equation above and was determined to be -2.67×10^{-7} C/cm^2 which was confirmed with the expected amount of charge on each bead.

Next, live and dead *Listeria innocua* were obtained as described earlier, and moved through the micropore under the application of an electric field. In addition, free bacteria measurements were also performed similar to the ones described for beads earlier. The live bacteria were moved from negative to positive potential and the heat-inactivated ones were moved from positive to negative potential. Figures 10 and 11 show the plot of translocation time and velocity versus applied electric field for live *Listeria innocua* through the pore, respectively. The decrease in translocation time as a function of increasing electric field magnitude clearly demonstrates that the bacteria are indeed moving through the

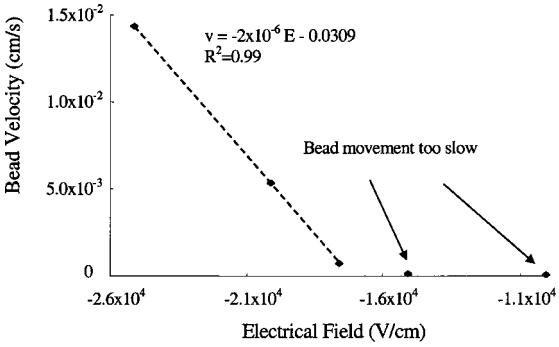

FIG. 8. Average velocity of beads through the pore vs the electric field. The negative mobility implies a negative charge. The slope of the line used to fit the first three points results in a mobility of -2×10^{-6} cm^2/V s.

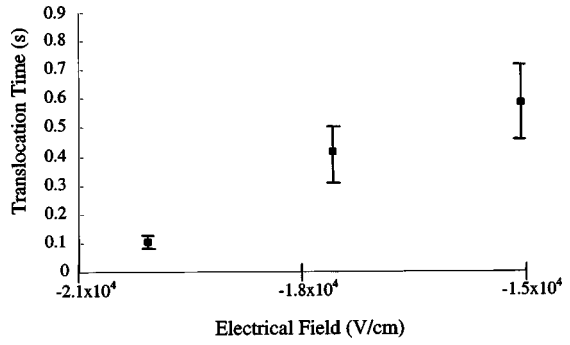

FIG. 10. Plot of translocation time of live *Listeria innocua* with pore vs applied electric field.

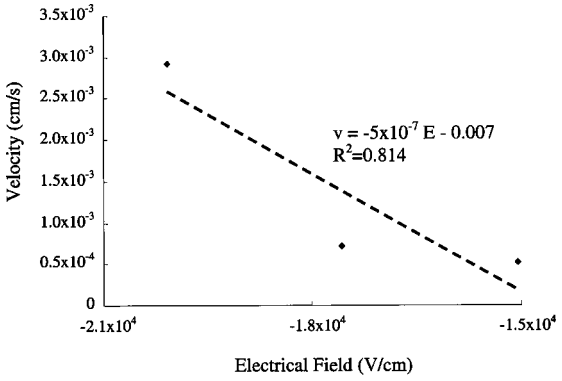

FIG. 11. Plot of velocity vs electric field for live *Listeria innocua* through the pore. The slope of the line used to fit the points results in a mobility of -5×10^{-7} cm^2/V s.

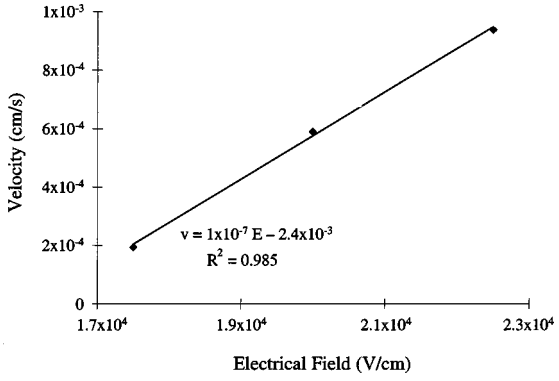

FIG. 13. Plot of velocity vs electric field for heat-inactivated *Listeria innocua* through the pore. The slope of the line used to fit the points results in a mobility of 1×10^{-7} cm^2/V s.

pore under a drift field. Figure 12 shows the plot of velocity versus applied electric field for live *Listeria innocua* without the pore. The data are much more consistent since individual organisms were tracked in the video and the electric field is also uniform. The mobility extracted from the velocity versus applied electric field for free live *Listeria innocua* is -3×10^{-4} cm^2/V s, which is very close to expected mobility of -4.5×10^{-4} cm^2/V s (Ref. 12) and -2.07×10^{-4} cm^2/V s (Ref. 15). (It should be noted that the results in Refs. 12 and 15 were for *Listeria monocytogenes* Scott A, and are expected to be similar for *Listeria innocua*.)

The least-square fit line through the data in Fig. 11 shows a fit factor of 0.814 and a wider variability in the measured data. This variability could be due to three possible factors. First, even though the movement of the bacteria through the pore is expected to be along its length, it is possible that the movement of the bacteria could be in other orientations, resulting in variability in the measured translocation times. Second, *Listeria innocua* is rod-shaped bacteria with about 0.5–1 μm in diameter and about 1–3 μm in length. The velocity was extracted using the measured translocation time and the length of the bacteria. The length used in the calculation of velocity was 3 μm, whereas the length of the bacterial cells can actually vary from 1 to 3 μm. Third and finally, the charge density on the surface of the bacteria could also vary resulting in a wider variation in the electrophoretic characteristics among individual bacterium. Figures 13 and 14 show the plots of velocity versus applied electric field for heat inactivated *Listeria innocua* with and without the pore, respectively. Based on the results from Fig. 2, the microorganism was moved from the positive to the negative electrode and hence it was further confirmed that the heat inactivated *Listeria innocua* is positively charged.

All of the above results are summarized in Table I and presented in Figs. 7–14. Some points are to be noted as discussed below.

(i) The values mobility for live *Listeria innocua* without the micropore is consistent with earlier published data and hence establishes the validity of the microscopic video measurements.

(ii) The heat-inactivated *Listeria innocua* have positive charges on the surface as confirmed by the electrophoresis measurements with and without the pore. The data on these dead bacteria are more consistent and the least square fit factors are closer to unity. The surface charge density for the case of the heat-inactivated *Listeria innocua* in the given pH, has not been reported and can be useful in a wide variety of practical applications.

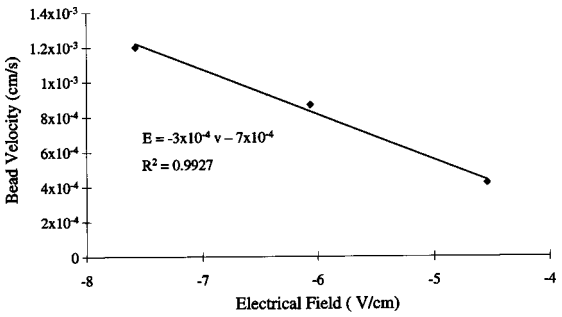

FIG. 12. Plot of velocity vs electric field for live *Listeria innocua* without pore. The slope of the line used to fit the points results in a mobility of -3×10^{-4} cm^2/V s.

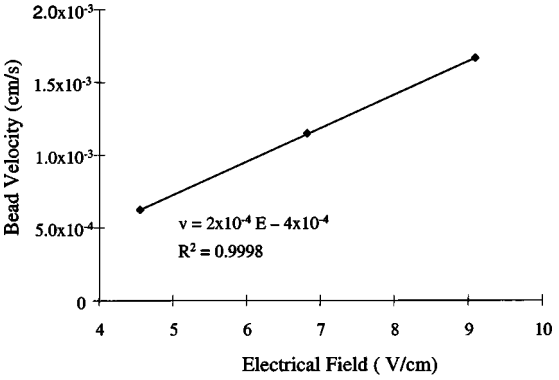

FIG. 14. Plot of velocity vs electric field for heat-inactivated *Listeria innocua* without pore. The slope of the line used to fit the points results in a mobility of 2×10^{-4} cm^2/V s.

TABLE I. Summary of the electrophoretic mobility of polystyrene beads, and live and heat-killed *Listeria innocua*.

	Mobility ($cm^2/V\,s$) (without pore)	Mobility ($cm^2/V\,s$) (with pore)	Charge (C/cm^2) (without pore)
Polystyrene beads	-2×10^{-4}	-2×10^{-6}	-2.7×10^{-7}
Live *Listeria innocua*	-3×10^{-4}	-5×10^{-7}	-3.5×10^{-7}
Dead *Listeria innocua*	$+2\times10^{-4}$	$+1\times10^{-7}$	$+2.7\times10^{-7}$

(iii) The differences between the mobility with and without the microfabricated pore are 2–3 orders of magnitude. For example, the mobility extracted from live *Listeria innocua* through the pore experiment (-5×10^{-7} $cm^2/V\,s$) is about 3 orders of magnitude lower than the free *Listeria innocua* mobility. Similar results are observed in the case with the beads. The difference is expected due to the higher hydrodynamic pressure experienced by the micro-organism (or bead) as it moves through the pore under the applied electric field. The entities move through the wider region of the channel and have velocities and mobility similar to the no-pore case. As the entities move closer to the pore, the velocity decreases due to the increased hydrostatic pressure within the narrow pore, even though the electric field is about 1–2 orders of magnitude higher (as confirmed by the ANSYS simulations). Once the organisms have traversed through the pore, the velocity is expected to increase again to values closer to the case of no-pore.

(iv) The surface charges on the beads are within the expected range. The surface charge on the live and heat-inactivated *Listeria innocua* (without the pore) was calculated approximately using the simplified Eq. (3) for a charged sphere. The radius used was the equivalent value for a sphere with the same surface area as that of a micro-organism with diameter of 0.5 μm and length of 3 μm. The same dimensions were used for the heat-inactivated bacteria.

This technique can possibly be used to devise a new single cell electronic detector by coating or attaching antibodies for specific micro-organisms and then measuring the translocation times through the pore. It can be postulated that since the micro-organisms slow down significantly when passing through the pore, enough time would be provided for the antigen/antibody interactions and hence, specific interactions will slow down the micro-organism even further. The device can also be used to study the interactions between a microfabricated surface and a charged entity.

VI. CONCLUSIONS

A simple microfabricated device has been fabricated to characterize the electrical properties such as charge of particles in buffer solution and to study the interactions between charged biological organisms and microfabricated surfaces and devices. The initial work was performed using negatively charged polystyrene beads and then live and dead *Listeria innocua* were used for the study. The device detects the passage of biological entities and provides an electronic output that indicates the velocity of the entity through a microfabricated pore. The device can be used to distinguish live bacteria from heat-inactivated ones since they have different surface charge properties and electrophoretic mobility. The electrophoretic mobility of the live and dead bacteria was also found to be about three orders of magnitude lower than data published in literature for the mobility of *Listeria* under similar pH and ambient without any pore or physical obstructions, and the difference was attributed to higher hydrostatic pressures within the narrow pore. Work is also ongoing to scale the pore size down in order for the device to be useful for the characterization of DNA and related molecules.

ACKNOWLEDGMENTS

The authors would like to thank H. Li for assistance in using the BAClight kit and Professor M. Ladisch for reviewing the manuscript and valuable discussion. We would also like to thank Dr. John Denton, D. Lubelski, Bill Crabill, and T. Miller of the microelectronics fabrication facility at Purdue University. H. Chang was funded through a Rockefeller Brothers Biomedical Pilot Initiative. A. Ikram was supported by the Center of Nano-scale Electronic/Biological Devices funded by the State of Indiana Research and Technology Fund.

The work was supported by Rockefeller Brothers Biomedical Pilot Grant, USDA, and the Center of Nano-scale Electronic/Biological Devices Funded by the State of Indiana Research and Technology Fund.

[1]R. Weinberger, *Practical Capillary Electrophoresis* (Academic, New York, 1993).
[2]O. Westerberg, J. Chromatogr. **480**, 3 (1989).
[3]E. Ogura, P. J. Abbati, and T. Morizumi, IEEE Trans. Biomed. Eng. **38**, 721 (1991).
[4]Y. Kikuchi, K. Sato, H. Ohki, and T. Kaneko, Microvasc. Res. **47**, 126 (1994).
[5]M. C. Tracey, R. S. Greenaway, A. Dass, P. H. Kaye, and A. J. Barnes, IEEE Trans. Biomed. Eng. **42**, 751 (1995).
[6]J. P. Brody, Y. Han, R. H. Austin, and M. Bitensky, Biophys. J. **68**, 2224 (1995).
[7]O. Bakajin, R. Carlson, C. F. Chou, S. Chan, C. Gabel, J. Knight, T. Cox, and R. H. Austin, Solid States Sensor and Actuator Workshop, Hilton Head, SC, 1998.
[8]U. Larsen, G. Blankenstein, and J. Branebjerg, Microchip Coulter Particle Counter, Transducers '97, 1997.
[9]H. E. Ayliffe, A. B. Frazier, and R. D. Rabbitt, J. Microelectromech. Syst. **8**, 50 (1999).
[10]F. Fuhr, U. Zimmermann, and S. G. Shirley, in *Electromanipulation of Cells* (CRC, Boca Raton), Chap. 5, pp. 259–328.
[11]M. Calderon-Miranda, G. V. Barbosa-Canovas, and B. G. Swanson, Int. J. Food Microbiol. **51**, 31 (1999).
[12]R. Briandet, T. Meylheuc, C. Maher, and M. N. Bellon-Fontaine, Appl. Environ. Microbiol. **65**, 5328 (1999).
[13]L. Boulos, M. Prevost, B. Barbeau, J. Coallier, and R. Desjardins, J. Microbiol. Methods **137**, 77 (1999).
[14]R. J. Hunter, *Zeta Potential in Colloid Science* (Academic, New York, 1981), p. 69.
[15]A. Mafu, D. Roy, and J. Goulet, J. Food Protect. **53**, 742 (1990).